

Validation of a *Drosophila* model of wild-type and T315I mutated BCR-ABL1 in chronic myeloid leukemia: an effective platform for treatment screening

Amani Al Outa,¹ Dana Abubaker,² Ali Bazarbachi,^{1,3} Marwan El Sabban,¹ Margret Shirinian² and Rihab Nasr¹

¹Department of Anatomy, Cell Biology and Physiology, Faculty of Medicine, American University of Beirut; ²Department of Experimental Pathology, Immunology and Microbiology, Faculty of Medicine, American University of Beirut and ³Department of Internal Medicine, Faculty of Medicine, American University of Beirut, Beirut, Lebanon



Haematologica 2018
Volume 105(2):387-397

ABSTRACT

Chronic myeloid leukemia (CML) is caused by a balanced chromosomal translocation resulting in the formation of *BCR-ABL1* fusion gene encoding a constitutively active BCR-ABL1 tyrosine kinase, which activates multiple signal transduction pathways leading to malignant transformation. Standard treatment of CML is based on tyrosine kinase inhibitors (TKI); however, some mutations have proven elusive particularly the T315I mutation. *Drosophila melanogaster* is an established *in vivo* model for human diseases including cancer. The targeted expression of chimeric human/fly and full human BCR-ABL1 in *Drosophila* eyes has been shown to result in detrimental effects. In this study, we expressed human BCR-ABL1^{p210} and the resistant BCR-ABL1^{p210/T315I} fusion oncogenes in *Drosophila* eyes. Expression of BCR-ABL1^{p210/T315I} resulted in a severe distortion of the ommatidial architecture of adult eyes with a more prominent rough eye phenotype compared to milder phenotypes in BCR-ABL1^{p210} reflecting a stronger oncogenic potential of the mutant. We then assessed the efficacy of the currently used TKI in BCR-ABL1^{p210} and BCR-ABL1^{p210/T315I} expressing flies. Treatment of BCR-ABL1^{p210} expressing flies with potent kinase inhibitors (dasatinib and ponatinib) resulted in the rescue of ommatidial loss and the restoration of normal development. Taken together, we provide a CML tailored BCR-ABL1^{p210} and BCR-ABL1^{p210/T315I} fly model which can be used to test new compounds with improved therapeutic indices.

Introduction

Chronic myeloid leukemia (CML) is a myeloproliferative neoplasm secondary to a precise cytogenetic abnormality involving a balanced chromosomal translocation between the Abelson murine leukemia (*ABL1*) gene on chromosome 9 and the breakpoint cluster region (*BCR*) on chromosome 22. This creates the (*BCR-ABL1*) fusion gene on chromosome 22 which encodes a constitutively active tyrosine kinase BCR-ABL.¹ Based on the breakpoints in BCR this translocation results in the formation of (p190, p210 and p230) fusion genes.² Overall, 95% of CML patients harbor the p210-kDa fusion protein, BCR-ABL1^{p210}.^{3,4} The BCR-ABL1 fusion oncoprotein increases the replication machinery and enhances cell growth which is mediated by downstream signaling pathways such as RAS, RAF, JUN kinase, MYC and STAT.⁵⁻¹¹

CML treatment was revolutionized with the development of tyrosine kinase inhibitors (TKI) which competitively inhibit the Adenosine triphosphate (ATP) binding site in the BCR-ABL1 kinase domain¹² and hence block the phosphorylation of proteins in the downstream signaling cascade. The first generation TKI (imatinib) showed major therapeutic improvement in the IRIS study (International Randomized Study of Interferon and STI571).¹³ However, imatinib success was

Correspondence:

MARGRET SHIRINIAN
ms241@aub.edu.lb

RIHAB NASR
rn03@aub.edu.lb

Received: February 15, 2019.

Accepted: May 16, 2019.

Pre-published: May 17, 2019.

doi:10.3324/haematol.2019.219394

Check the online version for the most updated information on this article, online supplements, and information on authorship & disclosures: www.haematologica.org/content/105/2/387

©2020 Ferrata Storti Foundation

Material published in *Haematologica* is covered by copyright. All rights are reserved to the Ferrata Storti Foundation. Use of published material is allowed under the following terms and conditions:

<https://creativecommons.org/licenses/by-nc/4.0/legalcode>.

Copies of published material are allowed for personal or internal use. Sharing published material for non-commercial purposes is subject to the following conditions:

<https://creativecommons.org/licenses/by-nc/4.0/legalcode>,

sect. 3. Reproducing and sharing published material for commercial purposes is not allowed without permission in writing from the publisher.



outsuited by the emergence of resistance caused by point mutations in the ABL1 kinase domain which necessitated the development of second-generation TKI.^{14,15} Dasatinib¹⁶⁻¹⁸ and nilotinib¹⁹⁻²¹ revealed faster and deeper molecular responses compared to imatinib in patients with newly diagnosed chronic phase CML. *In vitro*, dasatinib is more potent than imatinib²²⁻²⁴ and inhibits a wider spectrum of kinases including the Src family.²⁵ Nilotinib has a greater affinity than imatinib to the ATP binding site in BCR-ABL1 and its spectrum of kinase inhibition involves platelet-derived growth factor receptor (PDGFR) and c-Kit receptors.²⁶ Although nilotinib and dasatinib tackled the majority of imatinib-resistant mutations, neither of them targeted the T315I mutation (threonine to isoleucine substitution at position 315 in the ABL1 kinase domain) (BCR-ABL1^{T315I}).²³ Ponatinib, a third generation TKI, remains the only clinically available drug that is designed to overcome the T315I gatekeeper mutation.^{27,28} However, post-marketing safety issues with ponatinib involved serious cardiovascular events which led to its temporary suspension and then reintroduction with special patient recommendations.^{29,30}

In addition to the burden of resistance, therapy with TKI is hindered by their inability to eradicate leukemic stem cells and hence relapse often accompanies discontinuation of therapy.³¹ This fact imparts lifelong therapy with TKI despite accompanying side effects which result in ever-expanding costs for remission sustainment. Therefore, it seems evident that despite the breakthrough with TKI, CML remains a pathology that requires vigilant assessment of curative therapeutic interventions.

One simple, multicellular and genetically tractable animal model that has been exploited in recent years for modelling human diseases, including cancer, is *Drosophila melanogaster*.³² A myriad of advantages is held by this 3 mm long fruit fly as an *in vivo* model for dissecting the contribution of cellular mechanisms to human cancers and therapeutic screening. Fogerty *et al.* utilized *Drosophila* to decipher functional analogies between fly ABL1 and human BCR-ABL1 via neural-specific expression of p185 or p210 BCR-ABL1 transgenes. In these transgenes, BCR and the N-terminal sequences are derived from human oncogenes while the C-terminal ABL1 tail is from *Drosophila*. Both transgenes were capable to substitute the fruit fly ABL1 during axon genesis and flies expressing BCR-ABL1 revealed an increase in the phosphorylation of Enabled (Ena), a substrate for *Drosophila* Abl (dAbl). Expression of chimeric BCR-ABL1 in *Drosophila* eyes and CNS resulted in a rough eye phenotype and CNS developmental defects.³³ Furthermore, a recent study showed that the expression of human BCR-ABL1^{p210} in *Drosophila* activates the dAbl pathway and its upstream regulators Ena and Disabled (Dab).³⁴

In this study, we have overexpressed human BCR-ABL1^{p210} and mutated BCR-ABL1^{p210/T315I} in *Drosophila* compound eyes. BCR-ABL1^{p210/T315I} expression induced a significantly more severe rough eye phenotype compared to BCR-ABL1^{p210} pointing towards more aggressive tumorigenic capacities of the gatekeeper mutation. We have further assessed the efficiency of the current TKI used in clinics in modifying the characteristic eye phenotypes of transgenic flies. Dasatinib and ponatinib rescued the eye defects observed upon expression of BCR-ABL1^{p210} making this model a valuable screening platform to pre-clinically evaluate the efficacy of potential novel therapies for CML.

Methods

Fly stocks

Fly stocks were maintained at 25°C on standard agar-based medium. GMR-GAL4 (BDSC 1104) were obtained from Bloomington Stock Center. Treatment was performed at 18°C. Fly work was done following the institutional guide for the care and use of laboratory animals.

Generation of transgenic flies

Transgenic flies, harboring human BCR-ABL1^{p210} and BCR-ABL1^{p210/T315I} were generated using Phi C31 integrase system and were inserted in the 3rd chromosome for GAL4-UAS expression. BCR-ABL1^{p210} and BCR-ABL1^{p210/T315I} were inserted into pUAST-attB *Drosophila* expression vector (Custom DNA cloning). pUAST-attB-myc BCR-ABL1^{p210} and pUAST-attB-myc BCR-ABL1^{p210/T315I} were injected into y1 w67c23; P {CaryP} ABLattP2 (8622 BDSC) embryos to generate transgenic flies (BestGene Inc, Chino Hills, CA).

TKI administration

Imatinib (I-5577), nilotinib (N-8207), dasatinib (D-3307) and ponatinib (P-7022) were obtained from LC laboratories, MA, USA. Stock solutions were dissolved in DMSO and the required amount of TKI was added to instant *Drosophila* medium (Carolina Biological Supply Company). Since DMSO is known to be toxic to *Drosophila*,⁴⁰ 0.03% DMSO was used for low TKI concentrations and 0.3% for high concentrations.

Scoring of eye phenotypes and measurement of eye defect area

A grading score, that was modified from the score previously published,³⁵ was used for scoring and is based on the number of ommatidial fusions, the extent of bristle organization and ommatidial loss (*Online Supplementary Table S1*). For the measurement of the posterior eye defect area, Image J³⁶ was used. Scanning electron microscopy images were coded by one researcher and analysis was blindly performed by another researcher. N=20 flies from each genotype at each temperature were scored and the experiment was done in triplicate. For the measurement of posterior eye defect area an average of n=20-30 flies from each group was quantified and the experiment was done at least twice.

Scanning electron microscopy

Adult flies were fixed in 2% glutaraldehyde and 2% formaldehyde in phosphate buffered saline (PBS) (1x), washed, dehydrated with a series of increasing ethanol concentrations, dried with a critical point dryer (k850, Quorum Technologies), mounted on standard aluminum heads and coated with 20 nm layer of gold. Analysis was performed using Tescan, Mira III LMU, Field Emission Gun (FEG) scanning electron microscopy (SEM) with a secondary electron detector.

Western blot analysis

Fly heads were homogenized in Laemmli buffer and samples were loaded in 8% SDS-PAGE. Anti-ABL1 (SC-23, 1:1000, Santa Cruz Biotechnology, Santa Cruz, CA) and phospho-ABL1 (#2868, 1:500, Cell Signaling Technology) primary antibodies and anti-mouse (SC-2318, 1:5000, Santa Cruz Biotechnology, Santa Cruz, CA) and anti-rabbit (NA934, 1:5000, GE Healthcare) secondary antibodies were used for protein detection. An extract (150 µg) from 20-30 flies was used.

Statistical analysis

The statistical significance of the difference between the average scores of the rough eye phenotype and the average scores of

the posterior eye defect area was evaluated using two-way analysis of variance (ANOVA) followed by the Tukey's multiple comparisons test. One-way ANOVA was used when comparing the averages of the posterior eye defect area for dose response and was followed by Tukey's multiple comparisons test. Associations with $p < 0.05$ were considered significant. Statistical tests were done using GraphPad Prism 6.0 software.

Results

Expression of human BCR-ABL1 in *Drosophila* eyes induces transformation

To assess the transformative potential of human BCR-ABL1^{p210} and BCR-ABL1^{p210/T3151} in *Drosophila*, we expressed the transgenes in the adult eye using the glass-multimer reporter promoter GMR-GAL4 which drives the expression in all differentiating photoreceptor cells posterior to the morphogenetic furrow.³⁷ GMR-GAL4>w¹¹¹⁸ flies were used as a control. The temperature sensitivity of the GAL4-UAS system allowed us to the control BCR-ABL1 expression levels.³⁸ Therefore crosses were performed at 18°C, 25°C, and 29°C allowing for a reciprocal increase in transgene expression upon increased temperatures. Enclosed flies were imaged using light microscopy and SEM and evaluations of phenotypes were performed using a grading score (Online Supplementary Table S1) which graded the severity of the phenotype based on the extent of mechano-sensory bristles alignment, misplacement and duplication as well as the extent of ommatidial facets loss indicating the disruption in cellular proliferation and differentiation collectively defining interrupted normal development.³⁹ BCR-ABL1^{p210} and BCR-ABL1^{p210/T3151} showed a rough eye phenotype with increased severity at a higher temperature compared to control flies. At 18°C BCR-ABL1^{p210} and BCR-ABL1^{p210/T3151} flies exhibited a rough eye phenotype characterized by ommatidial fusions and areas of lost ommatidial facets, particularly at the posterior end of the eye, as well as multiple ectopic mechano-sensory bristles which are duplicated at some instances (Figure 1 B, F, J; Figure 2 B, F, J). At 25°C, a more severe rough eye was observed in both BCR-ABL1^{p210} and BCR-ABL1^{p210/T3151} with loss of the majority of ommatidial facets (Figure 1 D, H, L; Figure 2 D, H, L). At 29°C, the severity increased to involve the loss of the majority of mechano-sensory bristles in addition to the total loss of ommatidial facets in both BCR-ABL1^{p210} and BCR-ABL1^{p210/T3151} expressing flies (Figure 1 N, P, R; Figure 2 N, P, R). The average roughness of BCR-ABL1^{p210} significantly increased from 6.2 at 18°C to 8.2 ($P < 0.0001$) at 25°C and to 9.5 ($P < 0.0001$) at 29°C (Figure 1). As for BCR-ABL1^{p210/T3151}, the average roughness significantly increased from 6.6 at 18°C to 8.9 ($P < 0.0001$) at 25°C and to 10 ($P < 0.0001$) at 29°C (Figure 2). Western blot analysis confirmed the expression and phosphorylation of BCR-ABL1^{p210} and BCR-ABL1^{p210/T3151} in *Drosophila* eyes (Figure 3).

Dasatinib and ponatinib rescue human BCR-ABL1^{p210} mediated defects in *Drosophila*

Since expression of BCR-ABL1 at high temperature induced severe eye defects in adult flies, we opted to use the lowest temperature (18°C) which produced milder phenotypes for TKI screening efficiency allowing the easy visualization of any rescue due to drug activity. Four TKI were tested which included imatinib, nilotinib, dasatinib

and ponatinib. BCR-ABL1^{p210} flies were crossed to GMR-Gal4 flies and progeny were fed on multiple concentrations of the TKI (treated) or on DMSO alone (untreated). Untreated BCR-ABL1^{p210} and BCR-ABL1^{p210/T3151} flies showed the same defects described previously at 18°C focusing particularly on the posterior end of the eye with a characteristic defective area characterized by loss of ommatidial facets (Figures 4-6). The posterior eye defect area in untreated BCR-ABL1^{p210} flies showed an average of 4580 μm^2 and 4044 μm^2 on 0.03% DMSO and 0.3% DMSO respectively (Figures 4-6). On the other hand, untreated BCR-ABL1^{p210/T3151} expressing flies showed a wider area of defect at the posterior end with an average significant increase in the defect area to 11148 μm^2 ($P < 0.0001$) and 8728 μm^2 ($P < 0.0001$) on 0.03% DMSO and 0.3% DMSO respectively as compared to untreated BCR-ABL1^{p210} expressing flies (Figures 4-6).

Feeding 150 μM or 1500 μM imatinib to BCR-ABL1^{p210} expressing flies did not eliminate the posterior eye defect. However, the average posterior eye defect area showed a tendency to decrease with 1500 μM imatinib (3047 μm^2) as compared to that of 150 μM imatinib (4142 μm^2) and untreated flies (4044 μm^2) (Figure 4). Interestingly, the percentage of flies with total rescue (total disappearance of the posterior eye defect) with 150 μM and 1500 μM imatinib was 4% and 21% respectively. Similarly, feeding 28 μM (Online Supplementary Figure S1 E, K) or 280 μM (Online Supplementary Figure S1 F, L) nilotinib to BCR-ABL1^{p210} expressing flies did not eliminate the posterior eye defect. However, the average posterior eye defect area showed a tendency to decrease with 280 μM nilotinib (2480 μm^2) compared to that of 28 μM nilotinib (3871 μm^2) and untreated flies (4044 μm^2) (Online Supplementary Figure S1). The percentage of flies with total rescue with 28 μM and 280 μM nilotinib was 7% and 13% respectively.

Testing the potent TKI (dasatinib and ponatinib) showed more efficient rescue. Feeding 20 μM dasatinib or 280 μM ponatinib to BCR-ABL1^{p210} expressing flies improves the overall eye ommatidial arrangement and more specifically eliminates the characteristic posterior eye defect by restoring its normal ommatidial development (Figure 5 D, H; Figure 6 D, H). The average posterior eye defect area significantly decreased from 4580 μm^2 (in untreated flies) to 0 μm^2 ($P < 0.0001$) with 20 μM dasatinib (Figure 5) and from 4044 μm^2 (in untreated flies) to 267 μm^2 ($P < 0.0001$) with 280 μM ponatinib (Figure 6). The percentage of flies with total rescue was 100% with dasatinib and 86% with ponatinib.

A dose-response analysis for BCR-ABL1^{p210} expressing flies treated with dasatinib showed a significant decrease in the average posterior eye defect area from 4580 μm^2 in untreated flies to 2372 μm^2 ($P < 0.0001$) with 1 μM dasatinib, to 131 μm^2 ($P < 0.0001$) with 10 μM and to 0 μm^2 ($P < 0.0001$) with 20 μM dasatinib. The percentage of flies with total rescue increased from 25% to 92% and to 100% with 1 μM , 10 μM and 20 μM dasatinib respectively (Figure 7). Similarly, ponatinib also showed a dose-response whereby the average posterior eye defect area decreased significantly from 4044 μm^2 in untreated flies to 1684 μm^2 ($P < 0.0001$) with 28 μM and to 267 μm^2 ($P < 0.0001$) with 280 μM ponatinib (Figure 7). The percentage of flies with total rescue increased from 48% to 86% with 28 μM and 280 μM ponatinib respectively.

The BCR-ABL1^{p210/T3151} mutation is known to exhibit

resistance to imatinib, nilotinib and dasatinib in CML patients and this was confirmed in our model whereby the characteristic posterior eye defect did not show ommatidial rescue when feeding BCR-ABL1^{p210/T3151} expressing flies imatinib (Figure 4 Q, W, R, X), dasatinib (Figure 5 L, P) or nilotinib (Online Supplementary Figure S1

Q, W, R, X). However, feeding ponatinib to BCR-ABL1^{p210/T3151} expressing flies did not show the expected rescue of the posterior eye defect (Figure 6 L, P). Western blot analysis confirmed the expression and phosphorylation of BCR-ABL1^{p210} and BCR-ABL1^{p210/T3151} in *Drosophila* eyes from untreated or treated flies (Figures 5-6).

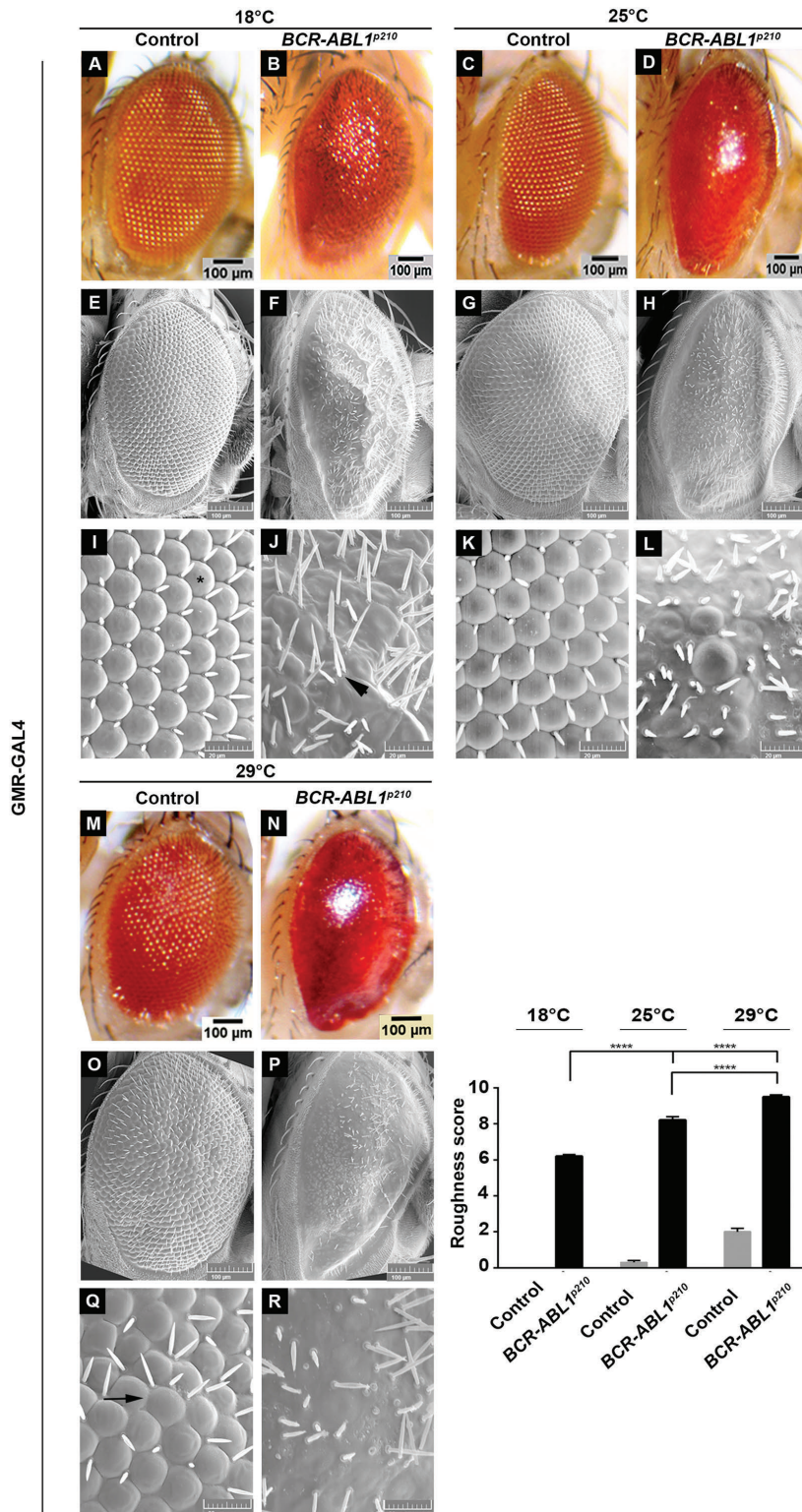


Figure 1. Rough eye phenotype induced by over-expression of human BCR-ABL1^{p210}. Light (A-D, M-N) and scanning electron (E-L, O-R) micrographs of adult *Drosophila* compound eyes expressing BCR-ABL1^{p210} under the control of the eye specific promoter GMR-GAL4. Flies were raised on 18°C (A, B, E, F, I, J) 25°C (C, D, G, H, K, L) or 29°C (M-R). I-L and Q-R are high magnifications of the centermost region of E-H and O-P respectively (1,370x). GMR-GAL4>w¹¹¹⁸ were used as control. Ommatidial facets are depicted in (I) by (*), misplaced mechanosensory bristles in (J) depicted by arrowheads and ommatidial fusions in (Q) are shown by arrow. Posterior is to the left. Lower right panel represents quantification of severity of roughness of the adult fly eye using a grading scale. Genotypes indicated are under the control of eye specific promoter GMR-GAL4. Data represents mean ± SEM. ****, P<0.0001.

Discussion

In this study, we established a transgenic *Drosophila* model expressing human BCR-ABL1 to serve as a credible platform for CML drug screening. Contrary to what has been done previously by Fogerty *et al.* where chimeric human/fly BCR-ABL1 was expressed in *Drosophila*³³ we expressed a full human BCR-ABL1^{p210} protein. In a recent

study, a CML *Drosophila* model expressing the human BCR-ABL1^{p210} was used to study genes and pathways that play a role in CML onset and progression.³⁴

The *Drosophila* eye, with its highly organized reiterative ommatidial structure, constitutes an efficient and relatively easy read out capable of amplifying subtle changes caused by disturbance to normal development. Therefore, we chose this epithelial monolayer as a target tissue for

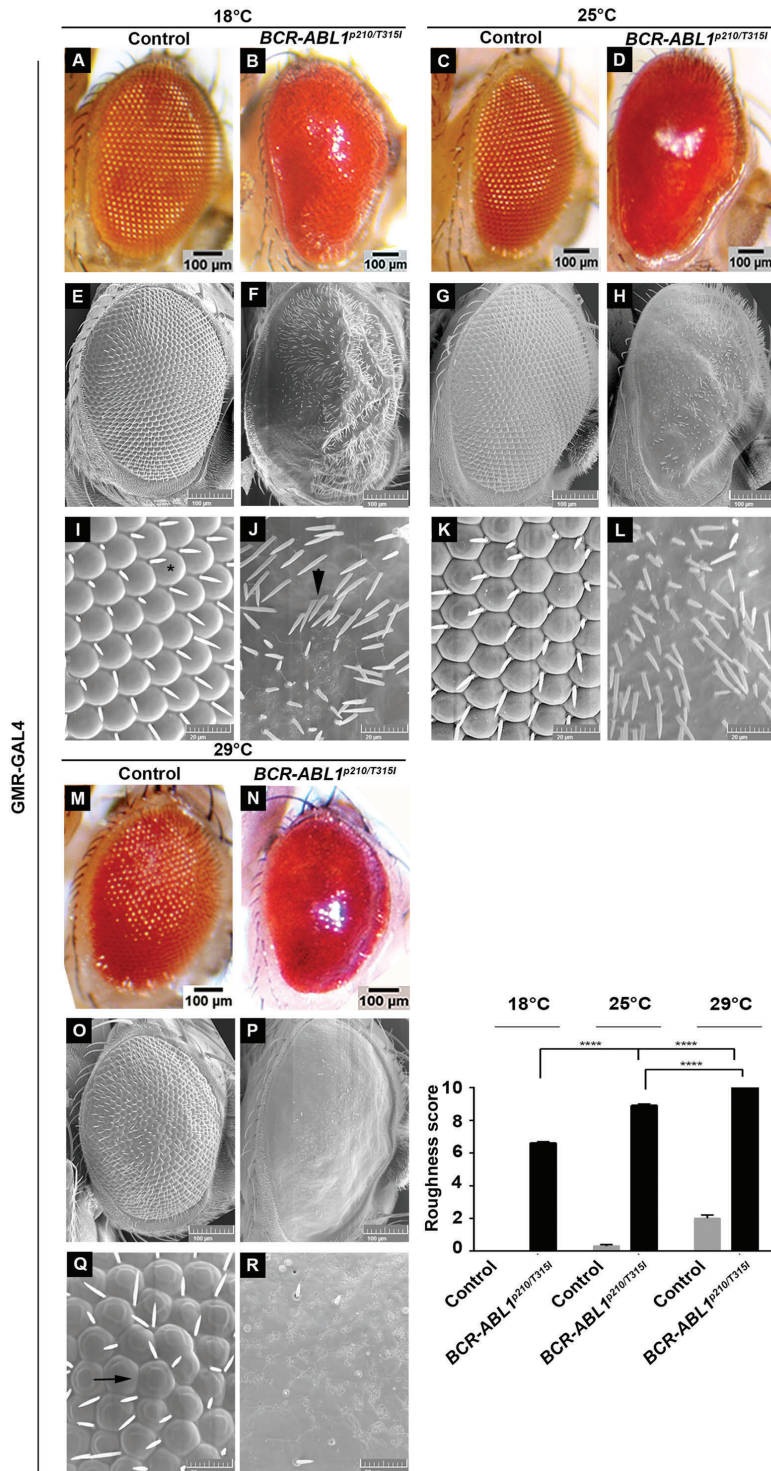


Figure 2. Rough eye phenotype induced by overexpression of human BCR-ABL1^{p210/T315I}. Light (A-D, M-N) and scanning electron (E-L, O-R) micrographs of adult *Drosophila* melanogaster compound eyes expressing BCR-ABL1^{p210/T315I} under the control of the eye specific promoter GMR-GAL4. Flies were raised on 18°C, 25°C or 29°C. I-L and Q-R are high magnifications of the centre region of E-H and O-P respectively (1,370x). GMR-GAL4>w¹¹¹⁸ were used as control. Ommatidial facets are depicted in (I) by (*), misplaced mechanosensory bristles in (J) depicted by arrowheads and ommatidial fusions in (Q) are shown by arrow. Posterior is to the left. Lower right panel represents quantification of severity of roughness of the adult fly eye using a grading scale. Genotypes indicated are under the control of eye specific promoter GMR-GAL4. Data represents mean ± SEM. ****, P<0.0001.

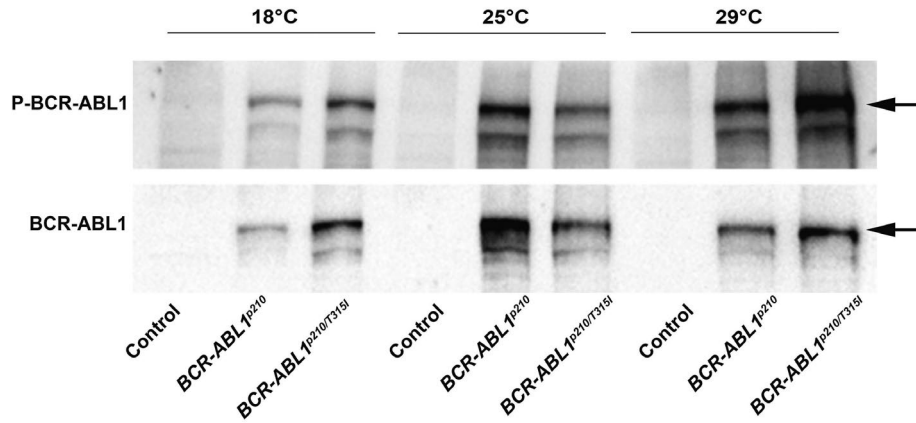


Figure 3. Expression of BCR-ABL1^{p210} and BCR-ABL1^{p210/T315I} in the compound eyes. Representative Western blot of the expression of BCR-ABL1 and phosphorylated levels in transgenic adult fly heads expressing BCR-ABL1^{p210} and BCR-ABL1^{p210/T315I} at different temperatures (18°C, 25°C, and 29°C). Genotypes indicated are under the control of eye specific promoter GMR-GAL4. GMR-GAL4>^{w¹¹¹⁸} were used as control.

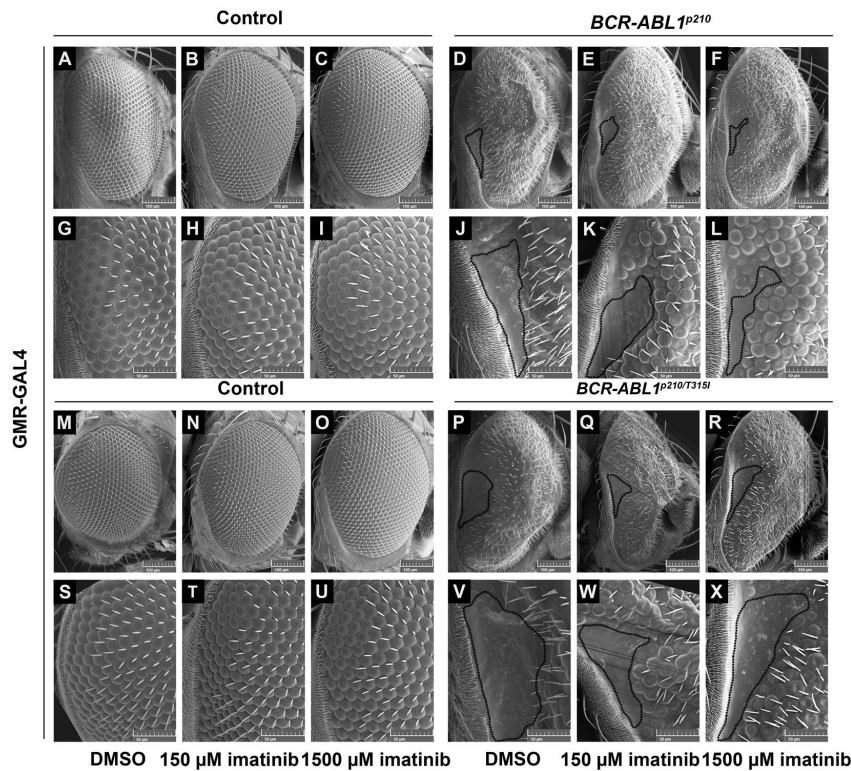
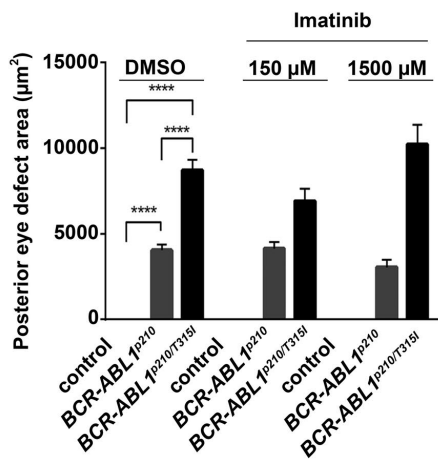


Figure 4. Imatinib shows a tendency to decrease BCR-ABL1^{p210} mediated eye defect. Scanning electron micrographs (A-X) of adult *Drosophila* compound eyes from flies fed on 0.3% DMSO only or imatinib. Posterior is to the left. GMR-GAL4>^{w¹¹¹⁸} were used as control. A-F are high magnification of the posterior end of the eye in G-L and S-X respectively (692 x). Normal development in control flies fed on DMSO or imatinib is observed. BCR-ABL1^{p210} (D, J) and BCR-ABL1^{p210/T315I} (P, V) expressing flies fed on DMSO show characteristic defective area with loss of ommatidial facets. Area is marked with a representative dashed line. Feeding low or high dose imatinib to BCR-ABL1^{p210} (E, K, F, L) and BCR-ABL1^{p210/T315I} (Q, W, R, X) retained the defective area in the posterior end of the eye marked with a dashed line. Compare to D, J and P, V respectively. Lower panel represents measurement of the posterior eye defect area (μm²). Data represents mean ± SEM. ****, P<0.0001.



expressing human BCR-ABL1^{p210} and human BCR-ABL1^{p210/T315I}. Bernardoni *et al.*³⁴ recently showed that expression of human BCR-ABL1^{p210} in *Drosophila* eyes was destructive to the normal eye development and resulted in a “glazy” eye phenotype as demonstrated by light microscopy images. We went further to investigate the effect of increased temperature on transgene expression as well as used SEM analysis in addition to light microscopy to show the subtle details of the eye phenotypes. Moreover, we opted to investigate whether one of the

most elusive BCR-ABL1 mutations (T315I) behaves similarly or differently to the wild type. We found that, with increased temperature, the rough eye phenotype was more prominent in T315I mutant BCR-ABL1 (Figures 1-2). To validate our model for treatment screening, we focused on a specific area in the posterior end of the eye which was evident to be defective in both BCR-ABL1^{p210} and BCR-ABL1^{p210/T315I} expressing flies. BCR-ABL1^{p210/T315I} expressing flies showed a more severe phenotype characterized by a wider defective area of lost ommatidial facets

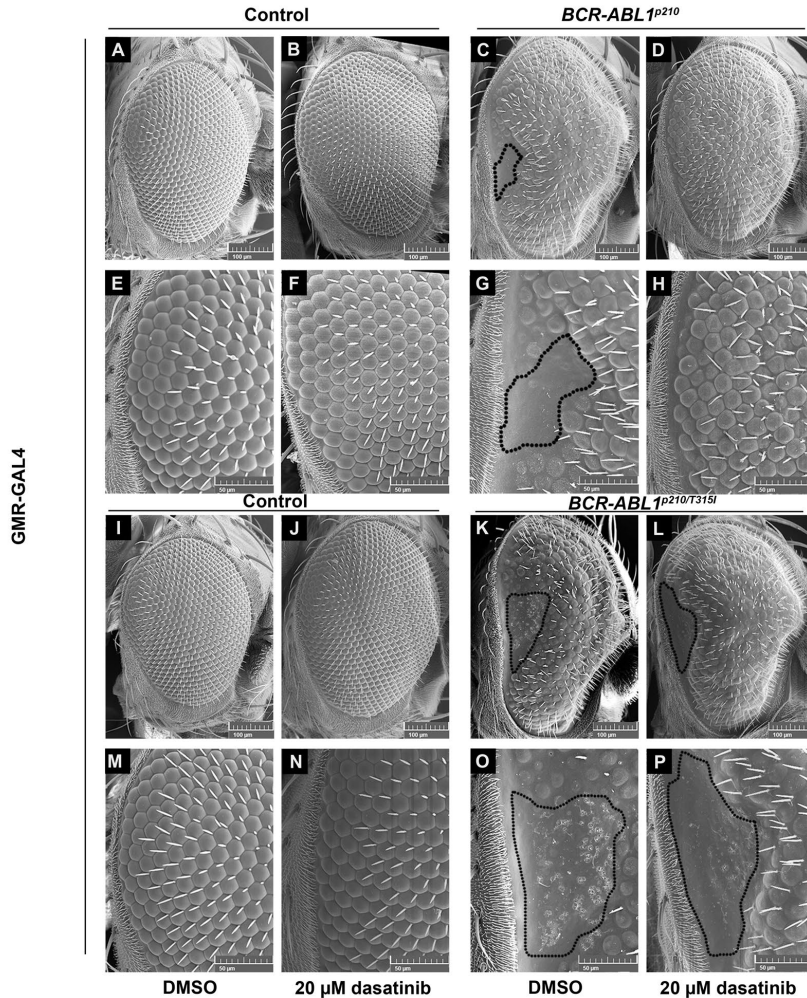
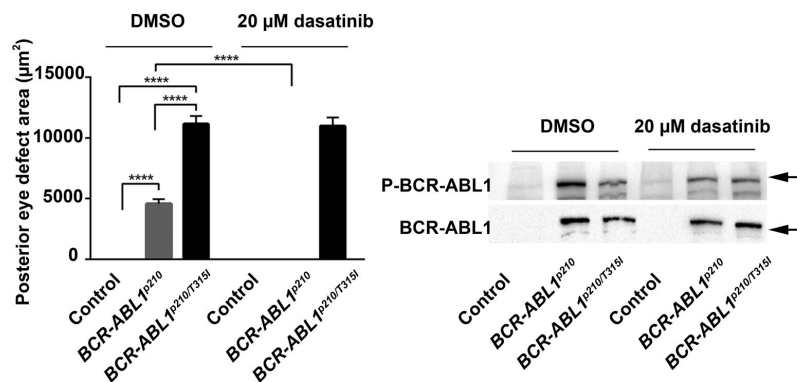


Figure 5. Dasatinib rescues BCR-ABL1^{p210} driven eye defect and shows target specificity *in vivo*. Scanning electron micrographs of adult *Drosophila* compound eyes from flies fed on 0.03% DMSO only or dasatinib. Posterior is to the left. GMR-GAL4>w¹¹¹⁸ were used as control. E-H and M-P are high magnification of the posterior end of the eye in A-D and I-L respectively (692x). Normal development in control flies fed on DMSO (A, E, I, M) or dasatinib is observed. BCR-ABL1^{p210} (C, G) and BCR-ABL1^{p210/T315I} (K, O) expressing flies fed on DMSO show characteristic defective area with loss of ommatidial facets. Area is marked with a representative dashed line. Ommatidial development in this area was restored with BCR-ABL1^{p210} flies fed on 20 μM dasatinib (D, H). Compare to (C, G). BCR-ABL1^{p210/T315I} flies showed no restoration of ommatidial development (L, P). Compare to (K, O). Lower left panel represents measurement of the posterior eye defect area (μm²). Data represents mean ± SEM. ****, P<0.0001. Lower right panel is a representative Western blot of the expression of BCR-ABL1 and phosphorylated levels in transgenic untreated and treated adult fly heads. Genotypes indicated are under the control of eye specific promoter GMR-GAL4.



as compared to flies expressing the wild type variant BCR-ABL1^{p210} indicating that the transformation capacity of T315I is much higher than the wild type BCR-ABL1^{p210}. Similar results were obtained when expressing BCR-ABL1^{p210/T315I} in other tissues where more detrimental effects were seen when compared to BCR-ABL1^{p210}. For example, expression of BCR-ABL1 in the fly imaginal discs resulted in pupal lethality with BCR-ABL1^{p210} expressing flies *versus* embryonic/larval lethality with BCR-ABL1^{p210/T315I} expressing flies (unpublished data).

We further validated the model by assessing the capability of the conventional treatments used in clinics for CML patients of improving the eye defects observed in the adult eyes of BCR-ABL1^{p210} and BCR-ABL1^{p210/T315I} flies. These TKI include imatinib as first generation TKI, nilotinib and dasatinib as second and ponatinib as third generation TKI. Dasatinib and ponatinib resulted in the full rescue of the BCR-ABL1^{p210} eye defect (Figures 5-6) in 100% and 86% of flies respectively. Imatinib and nilotinib (Figure 4; *Online Supplementary Figure S1*) exhibited a lower

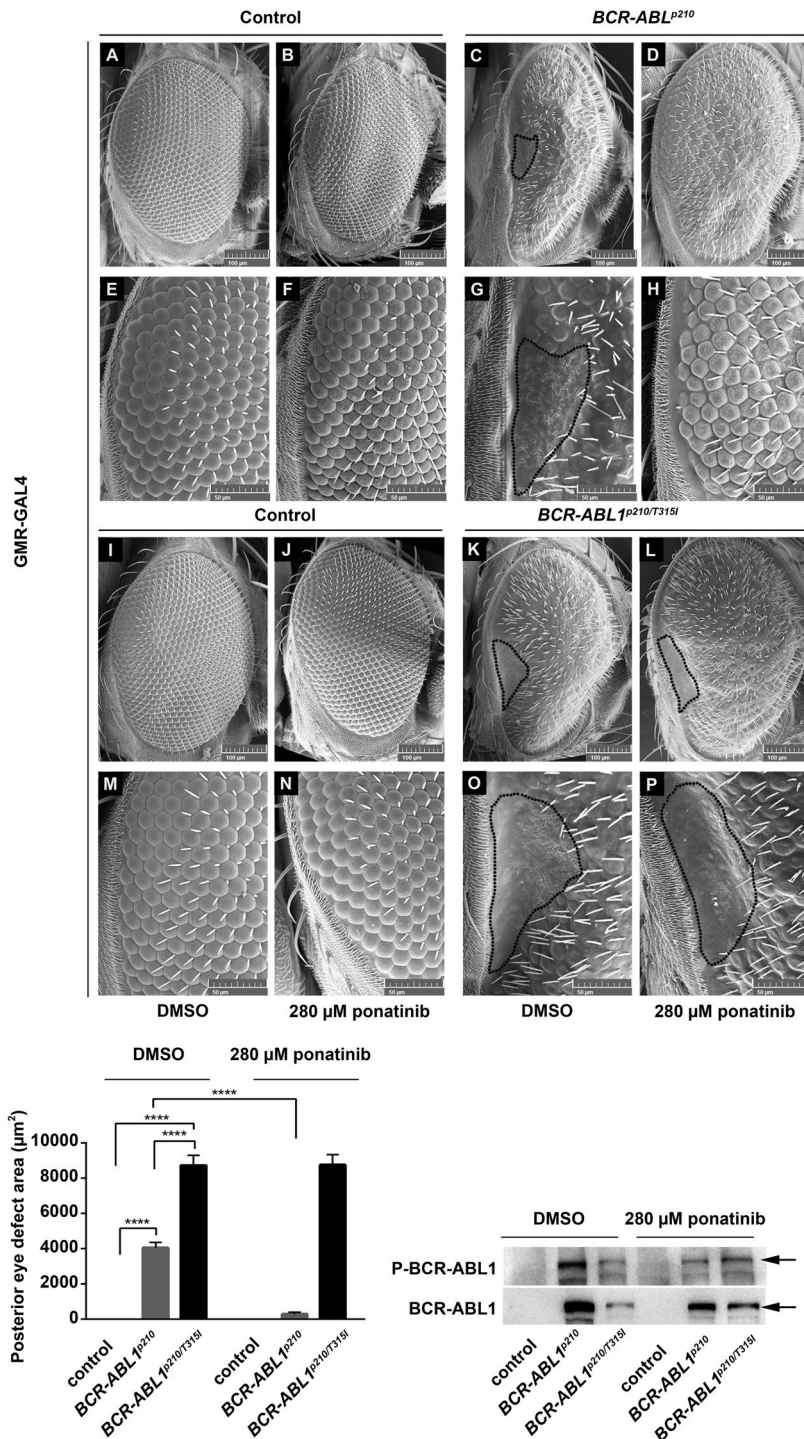


Figure 6. Ponatinib rescues BCR-ABL1^{p210} driven eye defect. Scanning electron micrographs of adult *Drosophila* compound eyes from flies fed on 0.3% DMSO only or ponatinib. Posterior is to the left. GMR-GAL4>w¹¹¹⁸ were used as control. E-H and M-P are high magnification of the posterior end of the eye in A-D and I-L respectively (692x). Normal development in control flies fed on DMSO or ponatinib is observed. BCR-ABL1^{p210} (C, G) and BCR-ABL1^{p210/T315I} (K, O) expressing flies fed on DMSO show characteristic defective area with loss of ommatidial facets. Area is marked with a representative dashed line. Ommatidial development in this area was restored with BCR-ABL1^{p210} flies fed on ponatinib (D, H). Compare to (C, G). BCR-ABL1^{p210/T315I} flies showed no restoration of ommatidial development (L, P). Compare to (K, O). Lower left panel represents measurement of the posterior eye defect area (μm²). Data represents mean ± SEM. *****, *P*<0.0001. Lower right panel is a representative Western blot of the expression of BCR-ABL1 and phosphorylated levels in transgenic untreated and treated adult fly heads. Genotypes indicated are under the control of eye specific promoter GMR-GAL4.

percentage of rescue, 21% and 13% respectively; this might be attributed to the difference in the drug potencies among to of imatinib and other TKI. Compared to imatinib, Dasatinib exhibits a 325-fold higher potency of BCR-ABL1 inhibition *in vitro* whereas nilotinib is only 20-fold more potent.²³ Another possible explanation for the limited rescuing efficacy of imatinib and nilotinib could be the activation of dAbl by BCR-ABL1 expression shown

previously by Bernardoni *et al.*,³⁴ which demonstrated that human BCR-ABL1 expression interferes with the dAbl signaling pathway and increases Ena phosphorylation, a dAbl target. On the other hand, using *Drosophila* wing epithelium as an *in vivo* model, Singh *et al.*⁴¹ demonstrated that activated dAbl exerts a positive feedback loop on *Drosophila* Src members leading to an increase in their activity and hence signal amplification. It is well known

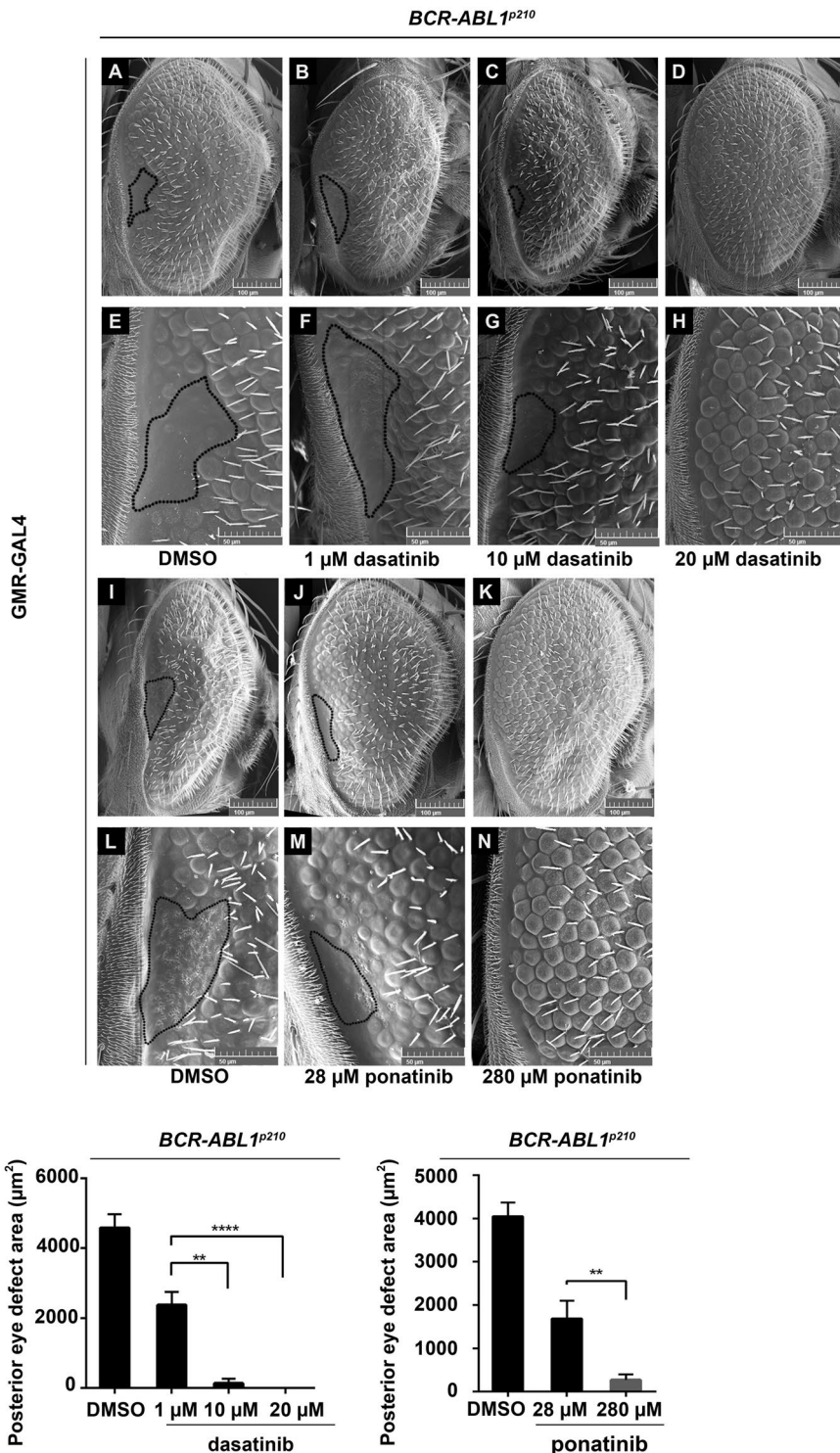


Figure 7. Dasatinib and ponatinib rescue BCR-ABL1^{p210} driven eye defect in a dose dependent manner. Scanning electron micrographs of adult *Drosophila* compound eyes from flies expressing BCR-ABL1^{p210} and fed on 0.03% DMSO (A, E), 1 μM (B, F), 10 μM (C-G) or 20 μM (D, H) dasatinib and flies fed on 0.3% DMSO (I, L), 28 μM ponatinib (J, M) or 280 μM ponatinib (K, N). Posterior is to the left. E-H and L-N are high magnification of the posterior end of the eye in A-D and I-K respectively (692x). Posterior eye defect area is marked with a representative dashed line. Lower panels represent measurement of the posterior eye defect area (μm²). Data represents mean ± SEM. ** *P*<0.01; **** *P*<0.0001.

that both dAbl⁴² and *Drosophila* Src⁴³ play important roles in *Drosophila* eye development; therefore it is possible that upon human BCR-ABL1 expression in *Drosophila* eyes, the dAbl signaling pathway is activated which in its turn activates *Drosophila* Src members and amplifies BCR-ABL1 mediated effects. Interestingly, Src is one of the kinases inhibited by dasatinib and ponatinib but not imatinib and nilotinib, therefore, this might possibly explain the more robust rescuing effect seen by dasatinib and ponatinib. Dasatinib demonstrated target specificity *in vivo* whereby BCR-ABL1^{p210/T3151} flies fed on dasatinib showed the expected resistance to treatment. BCR-ABL1^{p210/T3151} resistance to imatinib and nilotinib was also confirmed as there was no rescue of ommatidial development. In contrary to what was expected, ponatinib was not successful in rescuing progeny expressing BCR-ABL1^{p210/T3151}. While this phenomenon is hard to explain we would like to focus on the fact that the eye defect area was significantly larger upon BCR-ABL1^{p210/T3151} expression compared to the area upon BCR-ABL1^{p210} expression. Noting this significant increase in the average posterior eye defect area, we hypothesize that the phenotype was still very severe to allow for any drug reversal. Moreover, noting that the choice of the dose was limited by DMSO toxicity, the ponatinib dose used may not have been high enough to reverse the defect. On the other hand, we tried to test ponatinib to rescue the unpublished lethality phenotype of BCR-ABL1^{p210/T3151} flies; interestingly feeding ponatinib to BCR-ABL1^{p210/T3151} expressing flies rescued larval lethality and allowed development to

the pupal stage which suggests that the drug's response is tissue dependent. Feeding ponatinib or dasatinib to BCR-ABL1^{p210} expressing flies resulted in the rescue of pupal lethality and enclosure of adult flies (*unpublished data*).

We propose an *in vivo* model for BCR-ABL1 driven transformation where we show the efficacy of the current potent treatments in reversing a very subtle phenotype in a specific location in the posterior end of the adult compound eye. This system could be used to assess the efficacy of novel compounds by performing high throughput library testing *in vivo*. We believe that a *Drosophila* CML model to screen for potential compounds is required in this field especially as the currently used TKI do not target CML stem cells and hence are not curative.

Acknowledgements

MS and RN are funded by the National Council for Scientific Research-Lebanon (CNRS-L). AA is the recipient of CNRS-L/AUB Doctoral Scholarship award. We thank KAS Central Research Science Laboratory (CRSL) at the American University of Beirut (AUB) for their technical help in scanning electron microscopy imaging. The expert assistance from the DTS basic research core facilities at AUB is appreciated. We would like to thank Mr. Abdel Rahman Itani and Ms. Shireen Badini for their help in coding and scoring scanning electron microscopy images.

We acknowledge the Bloomington *Drosophila* Stock Center (NIH P40OD018537) for providing fly stocks.

We are sincerely grateful for the support of the Ferrata Storti Foundation.

References

- Rowley JD. Letter: A new consistent chromosomal abnormality in chronic myelogenous leukaemia identified by quinacrine fluorescence and Giemsa staining. *Nature*. 1973;243(5405):290-293.
- Jain P, Kantarjian H, Patel KP, et al. Impact of BCR-ABL transcript type on outcome in patients with chronic-phase CML treated with tyrosine kinase inhibitors. *Blood*. 2016;127(10):1269-1275.
- Shepherd P, Suffolk R, Halsey J, Allan N. Analysis of molecular breakpoint and mRNA transcripts in a prospective randomized trial of interferon in chronic myeloid leukaemia: no correlation with clinical features, cytogenetic response, duration of chronic phase, or survival. *Br J Haematol*. 1995;89(3):546-554.
- Groffen J, Stephenson JR, Heisterkamp N, de Klein A, Bartram CR, Grosveld G. Philadelphia chromosomal breakpoints are clustered within a limited region, bcr, on chromosome 22. *Cell*. 1984;36(1):93-99.
- Mandanas RA, Leibowitz DS, Gharehbaghi K, et al. Role of p21 RAS in p210 bcr-abl transformation of murine myeloid cells. *Blood*. 1993;82(6):1838-1847.
- Okuda K, Matulonis U, Salgia R, Kanakura Y, Druker B, Griffin JD. Factor independence of human myeloid leukemia cell lines is associated with increased phosphorylation of the proto-oncogene Raf-1. *Exp Hematol*. 1994;22(11):1111-1117.
- Raitano AB, Halpern JR, Hambuch TM, Sawyers CL. The Bcr-Abl leukemia oncogene activates Jun kinase and requires Jun for transformation. *Proc Natl Acad Sci U S A*. 1995;92(25):11746-11750.
- Sawyers CL, Callahan W, Witte ON. Dominant negative MYC blocks transformation by ABL oncogenes. *Cell*. 1992;70(6):901-910.
- Shuai K, Halpern J, ten Hoeve J, Rao X, Sawyers CL. Constitutive activation of STAT5 by the BCR-ABL oncogene in chronic myelogenous leukemia. *Oncogene*. 1996;13(2):247-254.
- Carlesso N, Frank DA, Griffin JD. Tyrosyl phosphorylation and DNA binding activity of signal transducers and activators of transcription (STAT) proteins in hematopoietic cell lines transformed by Bcr/Abl. *J Exp Med*. 1996;183(3):811-820.
- Ilaria RL, Jr., Van Etten RA. P210 and P190(BCR/ABL) induce the tyrosine phosphorylation and DNA binding activity of multiple specific STAT family members. *J Biol Chem*. 1996;271(49):31704-31710.
- Druker BJ, Talpaz M, Resta DJ, et al. Efficacy and safety of a specific inhibitor of the BCR-ABL tyrosine kinase in chronic myeloid leukemia. *N Engl J Med*. 2001;344(14):1031-1037.
- O'Brien SG, Guilhot F, Larson RA, et al. Imatinib compared with interferon and low-dose cytarabine for newly diagnosed chronic-phase chronic myeloid leukemia. *N Engl J Med*. 2003;348(11):994-1004.
- Jabbour E, Kantarjian HM, Saglio G, et al. Early response with dasatinib or imatinib in chronic myeloid leukemia: 3-year follow-up from a randomized phase 3 trial (DASISION). *Blood*. 2014;123(4):494-500.
- Larson R, Hochhaus A, Hughes T, et al. Nilotinib vs imatinib in patients with newly diagnosed Philadelphia chromosome-positive chronic myeloid leukemia in chronic phase: ENESTnd 3-year follow-up. *Leukemia*. 2012;26(10):2197-2203.
- Lombardo LJ, Lee FY, Chen P, et al.

- Discovery of N-(2-chloro-6-methylphenyl)-2-(6-(4-(2-hydroxyethyl)-piperazin-1-yl)-2-methylpyrimidin-4-ylamino)thiazole-5-carboxamide (BMS-354825), a dual Src/Abl kinase inhibitor with potent antitumor activity in preclinical assays. *J Med Chem.* 2004;47(27):6658-6661.
23. O'Hare T, Walters DK, Stoffregen EP, et al. In vitro activity of Bcr-Abl inhibitors AMN107 and BMS-354825 against clinically relevant imatinib-resistant Abl kinase domain mutants. *Cancer Res.* 2005;65(11):4500-4505.
 24. Tokarski JS, Newitt JA, Chang CY, et al. The structure of Dasatinib (BMS-354825) bound to activated ABL kinase domain elucidates its inhibitory activity against imatinib-resistant ABL mutants. *Cancer Res.* 2006;66(11):5790-5797.
 25. Shah NP, Tran C, Lee FY, Chen P, Norris D, Sawyers CL. Overriding imatinib resistance with a novel ABL kinase inhibitor. *Science.* 2004;305(5682):399-401.
 26. Weisberg E, Manley PW, Breitenstein W, et al. Characterization of AMN107, a selective inhibitor of native and mutant Bcr-Abl. *Cancer Cell.* 2005;7(2):129-141.
 27. Cortes JE, Kim D-W, Pinilla-Ibarz J, et al. Long-Term Follow-up of Ponatinib Efficacy and Safety in the Phase 2 PACE Trial. *Blood.* 2014;124(21):3135-3135.
 28. Cortes JE, Kim DW, Pinilla-Ibarz J, et al. A phase 2 trial of ponatinib in Philadelphia chromosome-positive leukemias. *N Engl J Med.* 2013;369(19):1783-1796.
 29. Breccia M, Pregno P, Spallarossa P, et al. Identification, prevention and management of cardiovascular risk in chronic myeloid leukaemia patients candidate to ponatinib: an expert opinion. *Ann Hematol.* 2017;96(4):549-558.
 30. Muller MC, Cervantes F, Hjorth-Hansen H, et al. Ponatinib in chronic myeloid leukemia (CML): Consensus on patient treatment and management from a European expert panel. *Crit Rev Oncol Hematol.* 2017;120:52-59.
 31. Mahon F-X, Réa D, Guilhot J, et al. Discontinuation of imatinib in patients with chronic myeloid leukaemia who have maintained complete molecular remission for at least 2 years: the prospective, multicentre Stop Imatinib (STIM) trial. *Lancet Oncol.* 2010;11(11):1029-1035.
 32. Gonzalez C. *Drosophila melanogaster*: a model and a tool to investigate malignancy and identify new therapeutics. *Nat Rev Cancer.* 2013;13(3):172.
 33. Fogerty FJ, Juang JL, Petersen J, Clark MJ, Hoffmann FM, Mosher DF. Dominant effects of the bcr-abl oncogene on *Drosophila* morphogenesis. *Oncogene.* 1999;18(1):219-232.
 34. Bernardoni R, Giordani G, Signorino E, et al. A new BCR-ABL1 *Drosophila* model as a powerful tool to elucidate pathogenesis and progression of chronic myeloid leukemia. *Haematologica.* 2019;104(4):717-728.
 35. Shirinian M, Kambris Z, Hamadeh L, et al. A Transgenic *Drosophila melanogaster* Model To Study Human T-Lymphotropic Virus Oncoprotein Tax-1-Driven Transformation In Vivo. *J Virol.* 2015;89(15):8092-8095.
 36. Schneider CA, Rasband WS, Eliceiri KW. NIH Image to ImageJ: 25 years of image analysis. *Nat Methods.* 2012;9(7):671-675.
 37. Freeman M. Reiterative use of the EGF receptor triggers differentiation of all cell types in the *Drosophila* eye. *Cell.* 1996;87(4):651-660.
 38. Duffy JB. GAL4 system in *Drosophila*: a fly geneticist's Swiss army knife. *Genesis.* 2002;34(1-2):1-15.
 39. Xin S, Weng L, Xu J, Du W. The role of RBF in developmentally regulated cell proliferation in the eye disc and in Cyclin D/Cdk4 induced cellular growth. *Development.* 2002;129(6):1345-1356.
 40. Cvetković VJ, Mitrović TL, Jovanović B, et al. Toxicity of dimethyl sulfoxide against *Drosophila melanogaster*. *Biol Nyssana.* 2015;6(2):91-95.
 41. Singh J, Aaronson SA, Mlodzik M. *Drosophila* Abelson kinase mediates cell invasion and proliferation through two distinct MAPK pathways. *Oncogene.* 2010;29(28):4033-4045.
 42. Xiong W, Rebay I. Abelson tyrosine kinase is required for *Drosophila* photoreceptor morphogenesis and retinal epithelial patterning. *Dev Dyn.* 2011;240(7):1745-1755.
 43. Takahashi F, Endo S, Kojima T, Saigo K. Regulation of cell-cell contacts in developing *Drosophila* eyes by Dsrc41, a new, close relative of vertebrate c-src. *Genes Dev.* 1996;10(13):1645-1656.